AN EXERGY ANALYSIS OF SOLAR-ASSISTED EJECTOR COOLING SYSTEM FOR DIFFERENT AREA RATIOS AT THEIR MAXIMUM COEFICIENTS OF PERFORMANCE VALUES

by

Fatih AKKURT [*] ***and Ali KAHRAMAN***

Department of Energy Systems Engineering,
Faculty of Engineering and Architecture Necmettin Erbakan University, Konya, Turkey

Original scientific paper
https://doi.org/10.2298/TSCI161027179A

In this paper, the exergy analysis of solar-assisted ejector cooling system was investigated with different ejector area ratios such as $A_r = 6.56$, $A_r = 7.17$, and $A_r = 7.86$. The analysis was performed on maximum COP values of each ejector area ratio based on the experimental results. The solar-assisted ejector cooling system was the combination of two subsystems including solar collector and ejector cooling. Exergy analysis was applied independently for each subsystem. The largest exergy destruction in cooling subsystem took place in the ejector followed by the generator, condenser, and evaporator, respectively. Exergy destruction proportions were 42.9%, 44.7%, and 45.2% in the ejector, 10.9%, 9.1%, and 10.1% in generator, 7.6%, 7.7%, and 8.7% in condenser, 5.9%, 5.6%, and 5.8% in evaporator of total cooling subsystem for different ejector area ratios. Although proportions were almost the same for each device, exergy destruction amounts increased with the increase of ejector area ratio.

Key words*: ejector cooling system, experimental, exergy analysis, maximum COP values*

Introduction

The increase in energy demand, accordingly reduction of conventional energy sources and environmental pollution increased the focus on RES. Solar energy seems the most promising among the RES. Recently the use of solar energy in cooling technology has a considerable attention. One of the cooling technologies that solar energy can be used is ejector cooling system which is possible to drive with low temperature energy sources. Solar-assisted ejector cooling systems (SAECS) have been investigated experimentally and theoretically by many researchers. Systems are generally intended for air conditioning and their COP values were obtained 0.3-0.8 while the temperature of the system collectors was between 80-150 °C by Abdulateef *et al.* [1]. It is a drawback for ejector cooling system, as their COP value of is less than the vapor-compression refrigeration systems. In order to minimize this negative situation, many types of research focused on loses of ejector cooling systems. Exergy analysis method was applied to these systems by many researchers to understand the magnitude and reasons of these loses.

Yan *et al.* [2] studied solar driven ejector compression heat pump cycle for air-source heat pump water heater application. They demonstrated that the largest exergy destruction is

[*] Corresponding author, e-mail: fakkurt@konya.edu.tr

generated in the ejector, which could amount to 25.7% of the total system exergy input, followed by condenser and evaporator. Chen *et al.* [3] investigated ejector performance characteristics in an ejector refrigeration cycle with refrigerants R600a, R245fa, and R141b. They also studied the amount of irreversibility generated in the ejector. They indicated the existence of an optimum generator temperature where the Carnot efficiency reaches to the maximum. Arbel *et al.* [4] showed that ejector irreversibility resulted from three factors including mixing, the kinetic energy losses, and the normal shock wave. Chen *et al.* [5] conducted an investigation of an ejector refrigeration system using conventional and advanced exergy analysis. Their results showed that highest exergy destruction takes place in the ejector and later the generator and the condenser. Sadeghi *et al.* [6] carried out an exergoeconomic analysis of ejector refrigeration cycle theoretically. They revealed that the generator has the highest exergy destruction followed by the ejector. Pridasawas and Lundqvist [7] investigated the solar-driven ejector refrigeration cycle by exergy analysis, most of the exergy destruction occur in the solar collector, followed by the ejector. They disclosed that an optimum generator temperature could be obtained for each evaporator temperature. Alexis [8] studied each of the components of the steam-ejector refrigeration system through exergy loss and coefficient of performance. The most exergy destruction was seen at ejector and later condenser of the system. Omidvar *et al.* [9] studied about the flow pattern in a variable geometry ejector used in a solar refrigeration system. They emphasized that the entropy generation in ejector was mainly caused by two factors: mixing and shock. Mixing phenomenon acts the main role when the temperature of the condenser is higher than the critical temperature. Conversely, shock event is majorly responsible when the condenser temperature is lower than the critical temperature. Ge *et al.* [10] presented an exergy analysis model of flat plate collectors. They examined the effects of ambient temperature, solar irradiance, fluid inlet temperature, and fluid mass-flow rate on useful heat rate, useful exergy rate, and exergy loss rate. According to their results, the exergy efficiency was 5.96%, and the largest exergy loss is caused by the temperature difference between the absorber plate surface and the sun, accounting for 72.86% of the total exergy rate.

As seen in literature surveys, there are a few experimental studies for such systems. The purpose of this study was to investigate exergy analysis of an SAECS based on the experimental results for different ejector area ratios such as $A_r = 6.56$, $A_r = 7.17$, and $A_r = 7.86$ at their maximum COP values. A group of experiments was performed by applying two axis tracking from east to west with 35° tilt angles at different collector areas. For all experiments condenser temperatures, T_c, was at a range of 26 °C and 28 °C while evaporator temperature, T_e, was kept at 8 °C. The most suitable collector areas are determined as $A_{sc} = 6.9$ m^2, $A_{sc} = 8.2$ m^2, and $A_{sc} = 9.2$ m^2 for $A_r = 6.56$, $A_r = 7.86$, and $A_r = 7.17$, respectively. Experiments were performed with suitable collector areas of each ejector area ratios. Optimum generator temperatures, maximum COP values, and cooling capacities were determined for each ejector configurations. Later, exergy analyses were applied at mentioned operation conditions. Exergy analysis was performed for solar collector subsystem and ejector cooling subsystem, but the main focus was on the ejector cooling subsystem.

Methodology

Experimental set-up and system performance

The SAECS was shown in fig. 1. The system consists of combination of two subsystems including solar collector and ejector cooling. While using water in the heating cycle, R123 refrigerant was used in ejector cooling cycle. The solar collector subsystem consisted of single-glazed and selective surface solar collectors. The solar energy system could be operated by

a variable number collectors with the valves placed between them. Main components of the ejector cooling system were a vapor generator, an ejector, a condenser, a receiver tank, an expansion valve, an evaporator and a pump.

The ejector is the most important device of the cooling system. The ejector configuration consisted of a supersonic nozzle, a mixing chamber with rounded entry, a constant area, and a conical diffuser. The operation of ejector device can be described: the primary vapor $\dot{m}_p$ at the high pressure leaving the generator enters the supersonic nozzle of the ejector; the very high-velocity vapor at the exit of the nozzle produces a high vacuum at the inlet of mixing chamber and entrains secondary vapor $\dot{m}_s$ into the chamber from the evaporator where it causes the pressure to decrease; the two streams first mix in the mixing chamber, and then, the pressure of the mixed stream rises to the condenser pressure in the diffuser; the mixed stream discharges from the ejector to the condenser where it condenses from a vapor to a liquid by rejecting heat to the surroundings. One part of the liquid refrigerant leaving the condenser enters the evaporator after passing through the expansion valve, and the other part flows to the liquid pump. The pressure of the liquid is increased to the generator pressure by the pump, and it is pumped to the generator to be vaporized again. The detailed information about the system can be found in Yapici *et al.* [11]

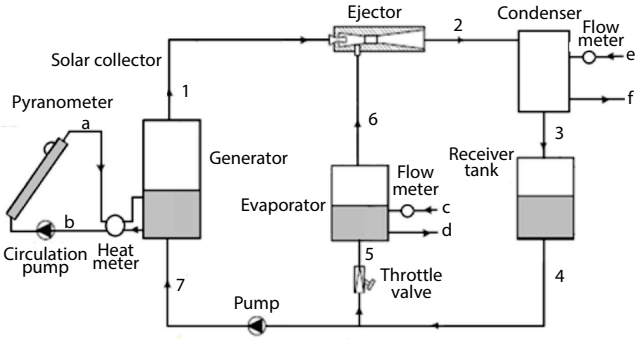

Figure 1. Solar-assisted ejector cooling system

Ejector area ratio is defined as the ratio of mixing chamber diameter, d_m, to nozzle throat diameter, d_t. The position of the supersonic nozzle is defined as the distance supersonic nozzle to the start of mixing chamber. Both parameters have great effects on the working conditions of ejector Yapici *et al*. [12]. In this study, three different ejector area ratios were obtained by changing mixing chamber diameter, while nozzle throat diameter was kept constant. The nozzle exit position was kept at 0- location for all experiments. The main parts and dimensions of the ejector configuration were illustrated at tab.1. while the ejector area ratios and their dimensions were presented on fig. 2.

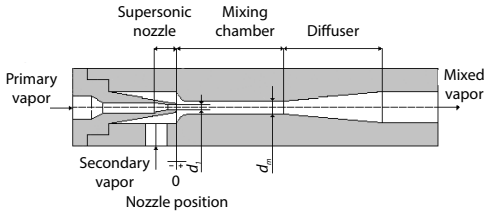

Figure 2. Ejector model

Table 1. Ejector area ratios and their dimensions

Ejector area ratio, A_r	Nozzle throat diameter, d_t [mm]	Mixing chamber diameter, d_m [mm]
6.56	3.21	8.22
7.17	3.21	8.60
7.86	3.21	9.00

During the experiments, a pyranometer was set on the collector to measure solar radiation. The pressures of the refrigerant were measured by pressure transmitters. The Pt100 sensors were used to measure all temperatures in the system. The flow rates $\dot{m}_{w,sc}$, outlet, inlet temperatures of solar collector T_a and T_b measured by a heat meter. The vaporization rate of the primary refrigerant, $\dot{m}_p$, at various generator temperatures in the nozzle was determined by measuring the time period of vaporization of a

defined liquid refrigerant volume in the generator. Heat inputs $\dot{Q}_{gen}$ and primary vapor flow rates $\dot{m}_p$, as a function of the generator temperature, were determined for throat diameter of 3.21 mm. Cooling water rate of condenser and chilling water rate of evaporator, $\dot{m}_{w,cond}$ and $\dot{m}_{w,eva}$, were measured by flow meters. Tap water was used as for both devices. The rate of the secondary refrigerant $\dot{m}_e$ was calculated with heat transfer equation between the refrigerant and chilling water after $\dot{Q}_{eva}$ was determined. Pressures in the system were measured with an accuracy of ±0.5 kPa while temperatures were measured with the accuracy of ±0.5 °C. The measurements of solar radiation and of heat input were performed with an accuracy of ±2.5% and ±0.6%, respectively. The flow rates were measured with an accuracy of ±0.1%.

The COP of the ejector cooling system was calculated by using the equation:

$$COP = \frac{\dot{Q}_{eva}}{\dot{Q}_{gen}} \tag{1}$$

where $\dot{Q}_{eva}$ and $\dot{Q}_{gen}$ is the cooling capacity and heat input to the vapor generator, respectively. They were calculated by using eqs. (2) and (3) as, $\dot{m}_s$ is the secondary vapor flow rate and $\dot{m}_p$ – the primary flow rate while h_1 and h_7 are the specific enthalpies of the refrigerant at the inlet and outlet of the generator, and $\dot{m}_{w,eva}$ is the flow rate, $T_{c,}$ and T_d are the temperatures of chilling water at the inlet and outlet of the evaporator:

$$\dot{Q}_{eva} = \dot{m}_{w,eva} c_p (T_c - T_d) \tag{2}$$

$$\dot{Q}_{gen} = \dot{m}_p (h_1 - h_7) \tag{3}$$

Exergy analysis

Exergy is the maximum work potential for a given form of energy with the environment taken as the reference state Kotas [13]. Energy analysis does not enough provide detailed information about internal losses, so exergy analysis can be preferred to determinate the losses in thermodynamic systems. For SAECS exergy analysis was applied independently for solar collector subsystem and an ejector cooling subsystem.

Exergy analysis of solar collector subsystem

Kalogirou *et al.* [14] presented a group of equations about exergy analysis of solar collectors. Exergy balance for solar collector subsystem was expressed with the following equation:

$$\dot{E}_{sc,in} + \dot{E}_{pump,cir} = \dot{E}_{sc,out} + I_{heat,trans} + I_{heat,loss} \tag{4}$$

where $\dot{E}_{sc,in}$ is the exergy input coming from solar radiation, $\dot{E}_{sc,out}$ – the exergy available at the outlet of the collector system, $I_{heat,trans}$ – the exergy destruction due to irreversible heat transfer in the solar collector, and $I_{heat,loss}$ – the exergy destruction due heat loss between the solar collector and ambient. The energy balance of solar collector expressed with the equation:

$$\dot{Q}_{sc,in} = \dot{Q} + \dot{Q}_o \tag{5}$$

where $\dot{Q}_{sc,in}$ is the energy flux coming from Sun, heat transfer in the solar collector, $\dot{Q}$ – the heat transfer rate in solar collector, and $\dot{Q}_o$ – the heat loss rate between collector and ambient. The energy flux coming from sun was expressed with the equation:

$$\dot{Q}_{sc,in} = \dot{q}^* A_{sc} \tag{6}$$

where, $\dot{q}^*$ is the solar radiation rate per meter square on the collector surface and A_{sc} is the solar collector area.

The $\dot{Q}_o$ is the collector-ambient heat loss rate and expressed with the equation:

$$\dot{Q}_o = U_L A_{sc}(T_{sc} - T_o) \tag{7}$$

where U_L is an overall heat transfer coefficient between the collector and the environment, T_o – the ambient temperature, and T_{sc} – the mean collector temperature. Heat transfer coefficient between the collector and the environment U_L, obtained 0.55 from the solar collector production company documentation. Exergy input coming from solar radiation was expressed with the equation:

$$\dot{E}_{sc,in} = \dot{Q}_{sc,in}\left(1 - \frac{T_0}{T^*}\right) \tag{8}$$

where T^* is approximately equal to 3/4 T_{Sun}, where T_{Sun} is the apparent black body temperature of the Sun, which is about 5770 K. Exergy destruction due to irreversible heat transfer in solar collector was expressed with the equation:

$$I_{heat,trans} = \dot{Q}_{sc,in} T_o\left(\frac{1}{T_{sc}} - \frac{1}{T^*}\right) \tag{9}$$

Exergy destruction due to irreversible heat loss between solar collector and ambient was expressed with the equation:

$$I_{heat,trans} = (\dot{Q}_{sc,in} - \dot{Q})\left(1 - \frac{T_0}{T_{sc}}\right) \tag{10}$$

Exergy input coming from circulation pump $\dot{E}_{pump,cir}$ was expressed with the equation:

$$\dot{E}_{pump,cir} = \dot{W}_{pump,cir} \tag{11}$$

where $\dot{W}_{pump,cir}$ is the value of the energy consumption at the pump to circulate the water between the solar collector and generator.

Exergy analysis of ejector cooling system

A group of equations was presented below to calculate exergy analysis of ejector cooling subsystem. Exergy balance for ejector cooling subsystem was expressed with the equation:

$$\dot{E}_{sc,out} + \dot{E}_{eva} + \dot{E}_{pump} = \dot{E}_{cond,out} + I_{total} \tag{12}$$

where $\dot{E}_{sc,out}$ was exergy input coming from solar collector, $\dot{E}_{eva}$ and $\dot{E}_{pump}$ was exergy inputs at the evaporator and pump, respectively. The $\dot{E}_{cond,out}$ was exergy output at the condenser and I_{total} was the sum exergy destruction of all devices constituting the cooling subsystem.

The I_{total} was expressed with the equation:

$$I_{total} = I_{gen} + I_{cond} + I_{eva} + I_{ejec} + I_{t,v} + I_{pump} + I_{rt} \tag{13}$$

Exergy destruction of generator I_{gen} was expressed with the equation:

$$I_{gen} = T_o\left[\dot{m}_p(s_1 - s_7) + \dot{m}_{w,sc}(s_b - s_a)\right] \tag{14}$$

where T_o was ambient temperature. Ambient temperatures were at about 25 °C for all three experiments. The $\dot{m}_p$ was the rate of primary refrigerant, s_7 and s_1 were entropy values of the

refrigerant at the inlet and outlet of the generator. The $\dot{m}_{w,sc}$ was the rate of water circulating in the solar collector, s_b and s_a were the entropy values of water at the inlet and outlet of the solar collector.

The I_{cond} was expressed:

$$I_{cond} = T_o\left[(\dot{m}_p + \dot{m}_s)(s_3 - s_2) + \dot{m}_{w,cond}(s_f - s_e)\right] \tag{15}$$

where $\dot{m}_p + \dot{m}_s$ were sum of the rates of primary and secondary refrigerant and s_2 and s_3 were entropy values of refrigerant at the inlet and outlet of condenser. The $\dot{m}_{w,cond}$ was the rate of cooling water, s_e and s_f were the entropy values of cooling water.

Exergy rate of evaporator $\dot{E}_{eva}$ was expressed:

$$\dot{E} = \dot{Q}_{eva}\left[1 - \left(\frac{T_0}{T_{w,eva}}\right)\right] \tag{16}$$

where $\dot{Q}_{eva}$ and $T_{w,eva}$ were cooling capacity and temperature of chilling water at evaporator.

The I_{eva} was expressed:

$$I_{eva} = T_o\left[\dot{m}_s(s_6 - s_5) + \dot{m}_{w,eva}(s_d - s_c)\right] \tag{17}$$

where s_5 and s_6 were entropy values of the refrigerant at the inlet and outlet of the evaporator. The $\dot{m}_{w,eva}$ was the rate of chilling water, s_c and s_d were the entropy values of chilling water. Inlet tab water temperatures were at about 20 °C for both condenser and evaporator.

Exergy destruction of ejector I_{ejec} was expressed:

$$I_{ejec} = T_o\left[(\dot{m}_p + \dot{m}_s)s_2 - \dot{m}_s s_6 - \dot{m}_p s_1\right] \tag{18}$$

where s_1 was the entropy value of refrigerant coming from the generator, s_6 was the entropy value of refrigerant coming from the evaporator, s_2 was the entropy value of refrigerant at the outlet of the ejector.

Exergy destruction of throttle valve I_{tv} was expressed:

$$I_{tv} = T_o\left[\dot{m}_s(s_5 - s_4)\right] \tag{19}$$

where s_4 and s_5 were the entropy values of refrigerant at the inlet and outlet of throttle valve.

Exergy rate of $\dot{E}_{pump}$ was expressed:

$$\dot{E}_{pump} = \dot{W}_{pump} \tag{20}$$

where $\dot{W}_{pump}$ was the value of the energy consumption at the pump.

Exergy destruction of pump I_{pump} was expressed:

$$I_{pump} = \dot{W}_{pump} + \dot{m}_p\left[(h_7 - h_4) - T_o(s_7 - s_4)\right] \tag{21}$$

where s_7, s_4 and h_7, h_4 were entropy and enthalpy values of the refrigerant at the inlet and outlet of the pump, respectively.

Exergy destruction of receiver tank I_{rt} was expressed:

$$I_{rt} = T_o\left[(\dot{m}_p + \dot{m}_s)(s_4 - s_3) + \frac{\dot{Q}_{rt}}{T_o}\right] \tag{22}$$

where s_3 and s_4 were the entropy values at the inlet and outlet of receiver tank and $\dot{Q}_{rt}$ was the heat transfer rate of receiver tank.

The $\dot{Q}_{rt}$ was expressed:

$$\dot{Q}_{rt} = (\dot{m}_p + \dot{m}_s)(h_4 - h_3) \tag{23}$$

where h_3 and h_4 were enthalpy values of the refrigerant at the inlet and outlet of receiver tank.

Results and discussion

In a cooling system, the system is required to operate at the maximum COP value. For ejector cooling systems for every area ratio, there is an optimum generator temperature where maximum COP could be obtained by Yapici *et al.* [12]. When the generator temperature reached to its optimum level the secondary vapor chokes at the inlet section of the mixing chamber. After which the cooling capacity remains constant.

Experiments were performed on three different days. Variations in the cooling capacities and COP values for different ejector area ratios were presented in figs. 3 and 4 by using all experimental data. Optimum generator temperatures, maximum COP values and cooling capacities were determined as 70 °C, 33.5%, and 756 W, 73.5 °C, 37%, and 950 W, 76 °C, 38.8%, and 1100 W for A_r = 6.56, A_r = 7.17, and A_r = 7.86, respectively, at their maximum COP values. Cooling capacities first increased with the increase of generator temperature and remained approximately constant after optimum generator temperature for all ejector configurations. On the other hand, COP values decreased with increasing of generator temperature due to the increase of solar radiation while the cooling capacity remained constant Akkurt [15].

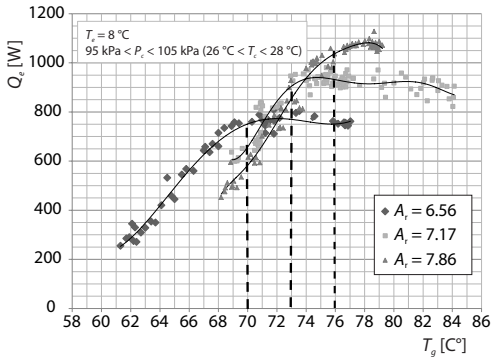

Figure 3. Variation in the cooling capacities for different ejector area ratios

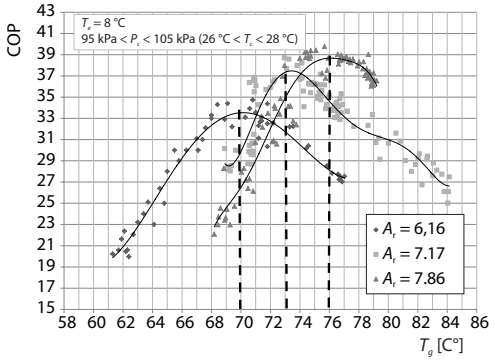

Figure 4. Variation in the COP for different ejector area ratios

For calculation of exergy analysis at solar collector subsystem solar radiations, ambient temperatures and mean collector temperatures at maximum COP for different applications were presented in tab. 2.

Table 2. Solar radiation values, ambient and mean collector temperatures of experiment configurations

Experiment configuration A_r / A_{sc} [m^2]	Solar radiation [Wm^{-2}]	Ambient temperature [°]	Mean collector temperature [°C]
6.56 / 6.9	950	25	76
7.17 / 8.2	940	24	83
7.86 / 9.2	960	25	85

The exergy input, output, and destructions in the solar collectors were calculated according to the eqs. (4)-(11). Exergy input of solar collector subsystem was provided by solar

radiation and circulation pump. The major amount of it was a reason of solar radiation when it was compared with a circulation pump. Although solar radiation values were different on different days, exergy input increased with the increase of the collector area. Total exergy input values were determined 6040 W, 7241 W, and 8290 W for $A_{sc} = 6.9$ m^2, $A_{sc} = 8.2$ m^2, and $A_{sc} = 9.2$ m^2, respectively.

A large proportion of exergy destructions were depending on the heat transfer in collector while a few of which were as a reason of heat loss from the collector to the ambient. Total exergy destruction values and their proportions were determined 5068 W and 84%, 5959 W and 83%, and 6796 W and 82% with respect to collector area, respectively. Although exergy destruction values increased quantitatively due to the increase of collector areas and temperatures, they were almost proportionally the same. The reasons for exergy destruction at solar collector was explained in some literature. Pridasawas and Lundqvist [7] stated that the exergy destruction caused by heat transfer in collector can be explained with two different events: the transformation of solar radiation to heat on the solar collector and the heat transfer from the solar collector to the working fluid. The majority of exergy destructions in collector was a reason of the temperature difference between the absorber plate surface and the Sun Ge *et al.* [10]. Another reason for the greatness of exergy destructions can be explained with the materials and types of solar collectors. If a better quality collector type, such as vacuum tube collectors were used instead of single-glazed and selective surface, exergy destructions would be less both quantitatively and proportionally Jafarkazemi *et al.* [16]. As it was seen in the results exergy destruction proportions were quite high, because solar collectors were commercial and low quality. So, experimental results confirm the comments in the aforementioned literature.

Exergy output is the amount difference between exergy input and exergy destruction both quantitatively and proportionally. Their values and proportions were determined 972 W and 16%, 1282 W and 17%, and 6796 W and 82% with the increase of collector area, respectively. Same as destruction values, exergy output values were also increased quantitatively with the increase of collector areas and temperatures but they were almost proportionally the same. Exergy output of solar collectors also constitutes a significant part of the input exergy of the ejector cooling subsystem. No scaled exergy balance diagrams for different collector areas were presented in fig. 5.

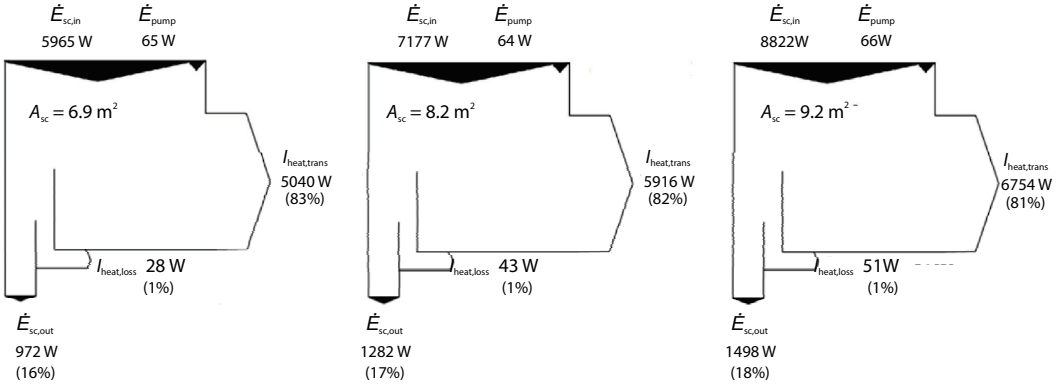

Figure 5. Exergy balance diagrams of solar collector subsystem for different collector areas

As results of the exergy calculations at the cooling subsystem, largest exergy destruction took place in the ejector followed by generator, condenser, evaporator and other devices, respectively. Exergy destruction portions were 42.9%, 44.7%, and 45.2% in the ejector, 10.9%,

9.1%, and 10.1% in generator, 7.6%, 7.7%, and 8.7% in condenser, 5.9%, 5.6%, and 5.8% in evaporator of total cooling subsystem for ejector area ratios $A_r = 6.56$, $A_r = 7.17$, and $A_r = 7.86$, respectively. The exergy destruction within throttling valve, pump and receiver tank were minuscule compared to overall system exergy destruction. No scaled exergy balance diagrams for different ejector area ratios were presented in fig. 6.

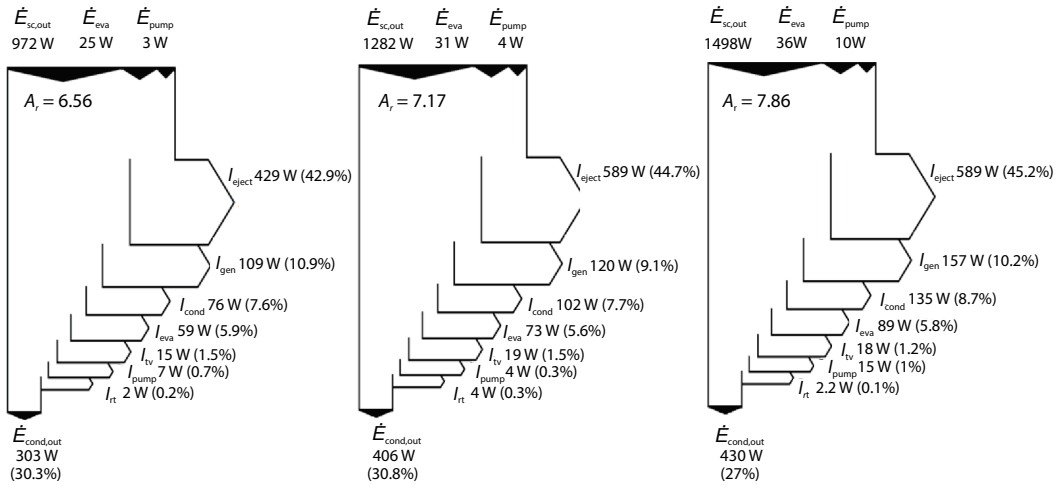

Figure 6. Exergy balance diagrams of cooling subsystem for different ejector area ratios

Ejector irreversibility was the results of three main factors: mixing of primary and secondary refrigerants, the kinetic energy losses, and the normal shock wave [4, 9]. In this study, the change of area ratio was only based on with the change of mixing chamber diameter. According to the results, it was seen that increase of exergy destruction portions were very small with the increase of area ratio. In the present study, the increase of exergy destruction values for different area ratios was a reason of increase of inlet and outlet temperatures in the ejector. The change of the ejector geometry in different ways can create different effects on exergy destruction values and rates. On the other hand, improving the design of the ejector in the refrigeration system will cause reductions in exergy destruction.

Exergy destructions of generator, condenser, and evaporator were based on entropy differences of the refrigerant at the inlet and outlet sections, the amount of heat transfer and structure of the device. In terms of these effects, second largest exergy destruction determined in generator followed by condenser and evaporator. As there was no change in the size and type of the generator, condenser and evaporator for different ejector area ratio, exergy destruction rates of each device was determined almost the same while the amount of exergy destruction increases with the increase of ejector area ratio. But, the improvement of the heat transfer efficiency of such devices and their proper selection for the system can cause reduction of the exergy destruction both in proportion and quantitative.

Conclusion

In this study, exergy analysis of SAECS was investigated at maximum COP values for different ejector area ratios. Experiments were performed with the suitable collector areas of each ejector configuration on different days. There was an optimum generator temperature where maximum COP could be obtained for each ejector configuration. Exergy analysis was

applied independently for solar collector subsystem and ejector cooling subsystem. Exergy balance diagrams were presented for each subsystem. Exergy destruction rates of each device were shown in the diagrams for different collector areas and ejector configurations. Exergy destruction in the collector is quite large depending on its quality. The use of better quality collector will reduce the proportion of destruction. The most considerable exergy destruction proportion in cooling subsystem was determined in the ejector followed by generator, condenser, and evaporator. Exergy destruction proportion of each device was almost the same for different area ratios while the amount of exergy destruction was increased. The difference of ejector area ratio was obtained by changing mixing chamber diameter while nozzle throat diameter was kept constant and the nozzle exit position was kept at 0- location. The change of ejector geometry and nozzle exit position in different ways will cause an effect on both amount and proportion of exergy destruction in the ejector.

References

[1] Abdulateef, J. M., *et al*., Review on Solar-Driven Ejector Refrigeration Technologies, *Renewable Sustainable Energy Reviews*, *13* (2009), 6-7, pp. 1338-1349
[2] Yan, G., *et al*., Energy and Exergy Efficiency Analysis of Solar Driven Ejector–Compressor Heat Pump Cycle, *Solar Energy*, *125* (2016), Feb., pp. 243-255
[3] Chen, J., *et al*., Parametric Analysis of Ejector Working Characteristics in the Refrigeration System, *Applied Thermal Engineering*, *69* (2014), 1-2, pp. 130-142
[4] Arbel, A., *et al*., Ejector Irreversibility Characteristics. *Journal of Fluids Engineering*, *125* (2003), 1, pp. 121-129
[5] Chen, J., *et al*., Conventional and Advanced Exergy Analysis of an Ejector Refrigeration System, *Applied Energy*, *144* (2015), Apr., pp. 139-151
[6] Sadeghi, M., *et al*., Exergoeconomic Analysis and Multi-Objective Optimization of an Ejector Refrigeration Cycle Powered by an Internal Combustion (HCCI) Engine, *Energy Conversion and Management*, *96* (2015), May, pp. 403-417
[7] Pridasawas. W., Lundqvist, P., An Exergy Analysis of a Solar-Driven Ejector Refrigeration System, *Solar Energy*, *76* (2004), 4, pp. 369-379
[8] Alexis, G. K., Exergy Analysis of Ejector-Refrigeration Cycle Using Water as Working Fluid, *International Journal of Energy Research*, *29* (2005), 2, pp. 95-105
[9] Omidvar, A., *et al*., Entropy Analysis of a Solar-Driven Variable Geometry Ejector Using Computational Fluid Dynamics, *Energy Conversion and Management*, *119* (2016), July, pp. 435-443
[10] Ge, Z., *et al*., Exergy Analysis of Flat Plate Solar Collectors, *Entropy*, *16* (2014), 5, pp. 2549-2567
[11] Yapici, R., Yetisen, C. C., Experimental Study on Ejector Refrigeration System Powered by Low Grade Heat, *Energy Conversion and Management*, *48* (2007), 5, pp. 1560-1568
[12] Yapici, R., *et al*., Experimental Determination of the Optimum Performance of Ejector Refrigeration System Depending on Ejector Area Ratio, *International Journal of Refrigeration*, *31* (2008), 7, pp. 1183-1189
[13] Kotas, T. J., *The Exergy Method of Thermal Plant Analysis*, Butterworths, London, 1985
[14] Kalogirou S. A., *et al*., Exergy Analysis of Solar Thermal Collectors and Processes, *Progress in Energy and Combustion Science, 56* (2016), Sept., pp. 106-137
[15] Akkurt, F., Experimental Investigation of a Solar-Assisted Ejector Cooling System at Different Ejector Area Ratios, *Journal of Selcuk University Natural and Applied Science*, *4* (2015), 4, pp. 20-32
[16] Jafarkazemi, F., *et al*., Energy and Exergy Efficiency of Heat Pipe Evacuated Tube Solar Collectors, *Thermal Science*, *20* (2016), 1, pp. 327-335

Paper submitted: October 27, 2016
Paper revised: August 8, 2017
Paper accepted: August 9, 2017